PHYSICAL REVIEW B
CONDENSED MATTER

THIRD SERIES, VOLUME 43, NUMBER 10 PART A 1 APRIL 1991

Energy-transfer processes in the $^1T_{2g}$ and $^3T_{2g}$ excited states of Ni^{2+}:MgO

R. J. Tonucci,* S. M. Jacobsen, and W. M. Yen*
Department of Physics and Astronomy, University of Georgia, Athens, Georgia 30602
(Received 1 October 1990)

A study of the decay curves of the $^1T_{2g} \rightarrow {}^3A_{2g}$ luminescence of Ni^{2+}:MgO at two different concentrations of Ni^{2+} (0.11 and 0.25 at. %) reveals a single exponential decay for the 0.11 at. % crystal and non-single-exponential decay for the 0.25 at. % crystal. This is interpreted in terms of transfer of excitation energy by cross relaxation. Fits of the nonexponential decay are most consistent with a dipole-quadrupole mechanism being responsible for the energy transfer. Examination of the oscillator strengths of the relevant Ni^{2+} transitions appears to support this notion, although the presence of an exchange interaction cannot be ruled out. Separate measurements on the $^3T_{2g} \rightarrow {}^3A_{2g}$ luminescence show that energy transfer from single ions to pairs also takes place. Two different types of Ni^{2+}-Ni^{2+} pairs are identified, nearest-neighbor ferromagnetic pairs with $2J = 2.5$ cm^{-1} and next-nearest-neighbor antiferromagnetic pairs with $2J = -35$ cm^{-1}.

I. INTRODUCTION

The optical properties of Ni^{2+}-doped MgO have attracted a great deal of interest in the literature.[1-3] In part, this interest has been driven by the system's promise as a near-infrared tunable solid-state laser.[4] Another aspect has been directed toward using the Ni^{2+}-dopant ions perfectly octahedral environment in the experimental testing of theoretical models of electronic energy levels and vibrational coupling.[5] More recently,[6,7] considerable effort has been employed in understanding the excited-state-absorption (ESA) properties of this system, as it has transpired that ESA is the limiting factor in the efficiency of many transition-metal-ion laser systems.

In this paper we present results on the energy-transfer (ET) properties of the system which show that, at high concentrations, two excited states are involved in quite different ET processes. The high-energy emitting level $^1T_{2g}$ has been shown to be involved in the transfer of excitation energy by cross relaxation in a number of Ni^{2+} systems, e.g., $KZnF_3$,[8] MgF_2,[9] as well as a number of chloride host lattices.[10] This type of cross relaxation is strongly concentration dependent and has the effect of making the decay curve of luminescence from $^1T_{2g}$ nonexponential and shorter than the decay curve observed in dilute crystals where cross relaxation is absent.[8] A necessary requirement for cross relaxation to take place is a resonance between emission bands from $^1T_{2g}$ and ground-state-absorption bands. Such a requirement is met in the aforementioned Ni^{2+} systems which show an overlap between the $^1T_{2g} \rightarrow {}^3T_{2g}$ band in emission and the $^3A_{2g} \rightarrow {}^3T^a_{1g}$ band in absorption. In the case of Ni^{2+}:MgO, the significantly larger value of the crystal-field parameter Dq in comparison with fluoride and chloride hosts, causes the $^3A_{2g} \rightarrow {}^3T^a_{1g}$ absorption band to shift to higher energy and, subsequently, the resonance condition with the $^1T_{2g} \rightarrow {}^3T_{2g}$ emission is lost. However, as we pointed out recently for Ni^{2+}:MgF_2,[11] and as has also been pointed out for the chloride hosts,[10] an overlap between the lower energy $^3A_{2g} \rightarrow {}^3T_{2g}$ absorption and the $^1T_{2g} \rightarrow {}^3T^a_{1g}$ emission may provide a second cross-relaxation pathway in Ni^{2+} systems. The $^1T_{2g} \rightarrow {}^1E_g, {}^3T^a_{1g}$ emission was recently measured for the MgO system by Payne,[7] and its spectral position indicates the presence of a strong resonance with the $^3A_{2g} \rightarrow {}^3T_{2g}$ absorption. The second cross relaxation should therefore be active for Ni^{2+}:MgO and we shall address this in the present paper.

As well as ET processes involving the $^1T_{2g}$ level, we will also explore processes from the $^3T_{2g}$ metastable first excited state. Using time-resolved fluorescence spectroscopy, it will be demonstrated that, in concentrated crystals, ET from single ions to pairs plays an important role in the relaxation. We will show that two different types of pairs can be identified on the basis of their ground-state splittings and quantitative estimates of the relevant ET rates will be made.

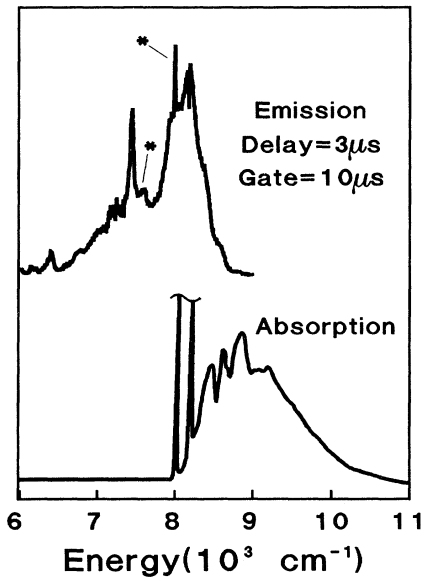

FIG. 1. Illustration of the overlap of the 2-K $^1T_{2g} \rightarrow {}^1E_g, {}^3T^a_{1g}$ emission and the $^3A_{2g} \rightarrow {}^3T_{2g}$ absorption of Ni^{2+}:MgO. Peaks marked by an asterisk are due to contamination from $^3T_{2g} \rightarrow {}^3A_{2g}$ emission as described in text.

II. EXPERIMENTAL SECTION

The Ni^{2+} concentrations were determined by measuring the absorption spectrum of the two crystals studied. The $^1T_{2g} \rightarrow {}^3A_{2g}$ luminescence was excited with a frequency-tripled Nd:YAG pumped dye laser, dispersed with a spex single monochromator and detected with a Varian VMP-159A cooled photomultiplier. In order to measure the $^1T_{2g} \rightarrow {}^1E_g, {}^3T^a_{1g}$ luminescence, a time-resolved experiment was necessary since this transition overlaps the $^3T_{2g} \rightarrow {}^3A_{2g}$ luminescence. Using a fast RCA $In_{1-x}Ga_xAs$ (rise time $=1.8$ μs) infrared detector, it was possible to obtain this spectrum with a delay of 3 μs and a gate width of 10 μs resulting in only slight contamination from the much longer-lived decay from $^3T_{2g}$ (see Fig. 1). Data acquisition of transients was obtained with a Data Precision D6100 multichannel analyzer and subsequent analysis was made on a microcomputer. The $^3T_{2g} \rightarrow {}^3A_{2g}$ luminescence was excited either with the fundamental Nd:YAG line or, in the case of selectively exciting Ni^{2+} single ions, with the second Stokes line of a dye-laser-pumped high-pressure H_2 Raman cell. The resulting luminsence was detected with the RCA $In_{1-x}Ga_xAs$ photodiode and recorded either with the multichannel analyzer or a boxcar averager. In all the experiments, cooling was achieved with a Janis Super Vari Temp helium-bath Dewar.

III. RESULTS

In all the experiments performed, two crystals of Ni^{2+}:MgO containing different concentrations of Ni^{2+} were used for comparative purposes. A dilute crystal containing 0.11 at.% Ni^{2+} (5.8×10^{19} ions/cm^3) was used to obtain the relevant single-ion parameter values from a system in which ET processes involving both $^1T_{2g}$ and $^3T_{2g}$ were absent. The more concentrated crystal, in which ET processes were evident, contained 0.25 at.% Ni^{2+} (1.3×10^{20} ions/cm^3).

In Fig. 1 spectral traces of the $^1T_{2g} \rightarrow {}^1E_g, {}^3T^a_{1g}$ emission and the $^3A_{2g} \rightarrow {}^3T_{2g}$ absorption at 2.0 K are shown, illustrating the degree of overlap or resonance. The measured overlap integral is found to be 1.5×10^{-4} (1/cm^{-1}). As alluded to in the Introduction, this is the criteria for energy transfer by cross relaxation. This process should be concentration dependent; since the probability of energy transfer increases as the average Ni^{2+}-Ni^{2+} separation in the bulk crystal decreases. The peaks marked by an asterisk in Fig. 1 are due to slight contamination of the $^1T_{2g} \rightarrow {}^1E_g, {}^3T^a_{1g}$ emission by the much longer-lived $^3T_{2g} \rightarrow {}^3A_{2g}$ emission, as the time resolution of the experiment could not completely exclude it.

Figure 2 shows an energy-level diagram for two Ni^{2+} ions, schematically illustrating the cross-relaxation mechanism that is likely to occur in Ni^{2+}:MgO. The process begins with one Ni^{2+} ion (the donor ion) in the $^1T_{2g}$ excited state and another (the acceptor ion) in the $^3A_{2g}$ ground state. In a simultaneous nonradiative process, the donor ion relaxes to ^1E_g or $^3T^a_{1g}$ and the acceptor ion is excited to $^3T_{2g}$. The net result is two excited Ni^{2+} ions created, at the expense of one excitation photon.

In Fig. 3 we examine the decay transients of the $^1T_{2g} \rightarrow {}^3A_{2g}$ green luminescence after pulsed excitation into the $^3A_{2g} \rightarrow {}^3T^b_{1g}$ absorption. The upper trace was obtained for the dilute crystal and is well described by a single exponential. The solid line is a best fit and corresponds to a lifetime of 42 μs. We note that this lifetime is somewhat longer than the 27 μs previous reported for this system.[7] The lower trace in Fig. 3 was obtained from

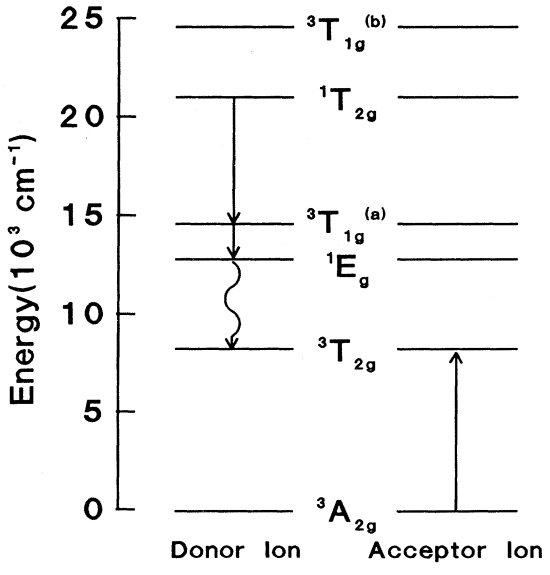

FIG. 2. Schematic illustration of the cross-relaxation pathway in Ni^{2+}:MgO.

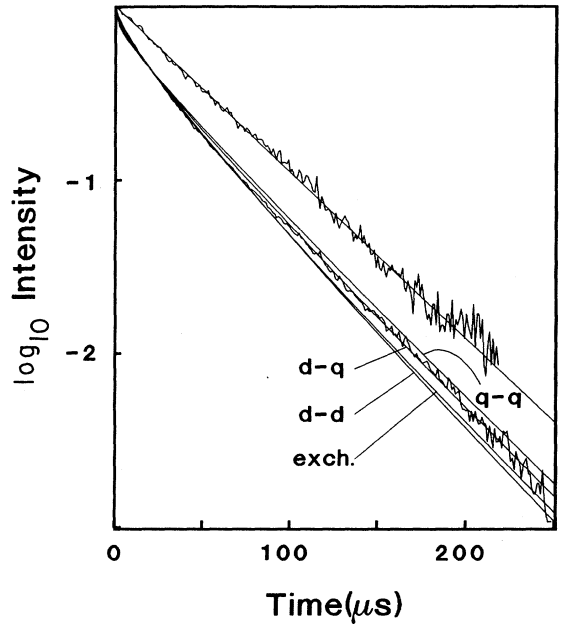

FIG. 3. Upper trace: $^1T_{2g}$ decay observed in 0.11 at. % Ni^{2+}:MgO crystal, with the solid line showing the fit to the single exponential ($\tau=42$ μs). Lower trace: $^1T_{2g}$ decay observed in 0.25 at. % Ni^{2+}:MgO crystal, with the solid lines representing fits to the dipole-dipole (*d-d*), dipole-quadrupole (*d-q*), quadrupole-quadrupole (*q-q*), and exchange (exch.) mechanisms, as described in Sec. IV A.

the concentrated crystal and clearly deviates from a single exponential. Nonexponential decays are indicative that cross relaxation is indeed taking place. A "best fit" of a single exponential to the lower trace yielded a lifetime of 26 μs, and we conclude that the previously reported result, which was obtained from a crystal of the same concentration as our 0.25% crystal, must have included cross-relaxation effects. We have previously pointed out the need to measure the intrinsic single-exponential decays on very lightly doped crystals for the Ni^{2+}:MgF_2 system.[11] The solid lines through the lower transient of Fig. 3 are fits to various multipolar and exchange models of ET by cross relaxation. The results of these fits, along with the relevant mechanisms and parameters, will be fully analyzed and discussed in Sec. IV A.

Figure 4 shows a comparison of the $^3T_{2g}$ emission spectra around the origin region for both concentrations, with traces taken at early and late times for the concentrated crystal. Excitation was made into the broad $^3T_{2g}$ absorption sideband with a pulsed 1.064-μm laser. The spectra show a dramatic concentration dependence. Besides the single-ion zero-phonon line at 8003 cm^{-1}, the more concentrated crystal shows two new sets of lines, one pair at 7999 and 7994 cm^{-1} and another at 7918 and 7883 cm^{-1}. Further, the time-dependent spectra of the concentrated crystal clearly indicate that energy transfer is taking place to the new sets of lines, at the expense of the single-ion luminescence.

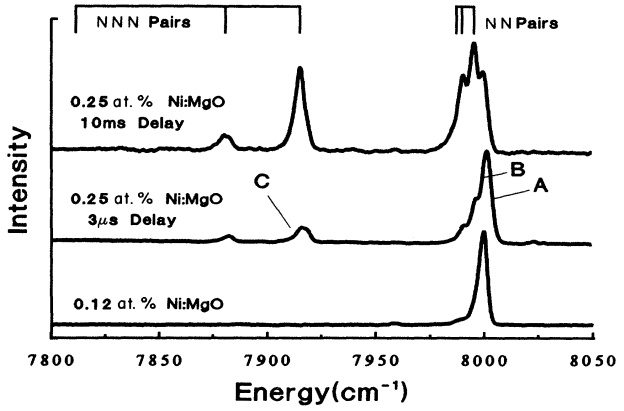

FIG. 4. $^3T_{2g} \rightarrow {}^3A_{2g}$ emission spectra at 2 K around the origin regions, for both concentrations of Ni^{2+}:MgO. Time-resolved spectra of 0.25 at. % crystal illustrates ET to pairs at late times.

Manson[2] had previously noted the presence of the 7918- and 7883-cm^{-1} lines and suggested that they might originate from Ni^{2+}-Ni^{2+} pairs. Later on, Grinvalds and Mironova[12] assigned these lines to an antiferromagnetically coupled Ni^{2+}-Ni^{2+} pair, but did not consider the geometrical arrangement of this pair in the MgO host, and failed to observe the lines at 7999 and 7994 cm^{-1}.

Figure 5 shows a schematic of the MgO crystal structure, illustrating two possible arrangements for Ni^{2+}-Ni^{2+} pairs. The correlations of these two types of pairs with the two sets of new lines observed in the concentrated crystal will be discussed in Sec. IV B. The decay tran-

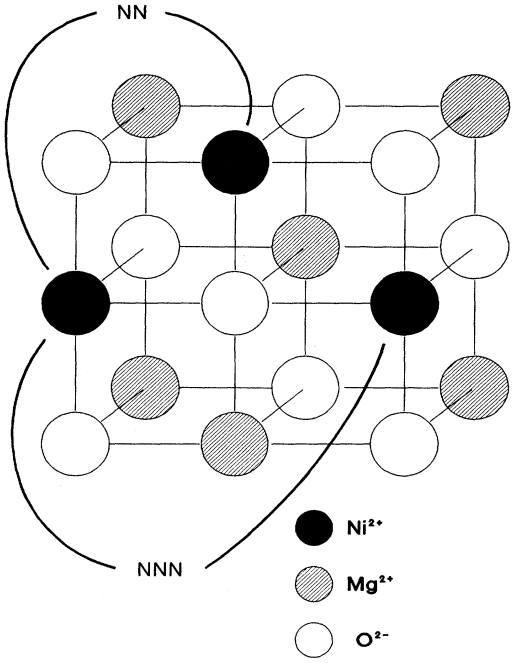

FIG. 5. Crystal structure of MgO, illustrating two different types of Ni^{2+}:Ni^{2+} pairs.

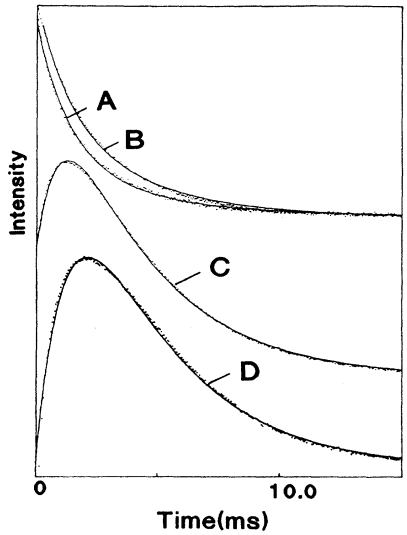

FIG. 6. Decay transients of $^3T_{2g} \rightarrow {}^3A_{2g}$ emission (2 K) from 0.25 at.% Ni^{2+}:MgO. Transients *A*, *B*, and *C* were obtained from positions *A*, *B*, and *C*, respectively, of Fig. 4 after pulsed excitation into the broad $^3A_{2g} \rightarrow {}^3T_{2g}$ absorption sideband. Transient *D* was obtained from position *C* of Fig. 1 after selective excitation into the $^3A_{2g} \rightarrow {}^3T_{2g}$ single-ion zero-phonon band. The solid lines are fits discussed in Sec. IV C.

sients obtained after 1.064-μm excitation at the energy positions denoted by *A*, *B*, and *C* in Fig. 1 are given in Fig. 6. Transient *D* of Fig. 6 was obtained by exciting the single-ion zero-phonon absorption at 8003 cm^{-1} with a tunable narrow-band laser, and observing at position *C* of Fig. 1. The solid lines are fits to a theoretical model which is discussed in Sec. IV C.

IV. DISCUSSION

A. Energy transfer $^1T_{2g}$ (cross relaxation)

The overlap of the $^1T_{2g} \rightarrow {}^1E_g, {}^3T_{1g}^a$ emission with the $^3A_{2g} \rightarrow {}^3T_{2g}$ absorption and the nonexponential decay found in the 0.25 at.% crystal have led us to conclude that cross relaxation is taking place. Theoretical treatments of the mechanism responsible for cross relaxation have previously been presented for the systems Ni^{2+}:$KZnF_3$ (Ref. 8) and Ni^{2+}:MgF_2.[9] In both cases the conclusion was reached that an exchange mechanism was likely responsible, although contributions from multipolar mechanisms could not be ruled out. As was already pointed out in Sec. III, however, the present system differs from the fluoride systems in that there is no resonance between $^1T_{2g} \rightarrow {}^3T_{2g}$ and $^3A_{2g} \rightarrow {}^3T_{1g}^a$. The mechanism responsible for cross relaxation in the oxide therefore need not necessarily be the same, since it depends on the relative oscillator strengths of different transitions if multipolar mechanisms are relevant. Further, the $^1T_{2g} \rightarrow {}^3T_{1g}^a / {}^3A_{2g} \rightarrow {}^3T_{2g}$ channel was not explicitly considered in the previous treatments of fluorides, and neglecting it may have led to erroneous conclusions concerning the parameter values and the subsequent mechanism.

We now turn to a discussion of the present system and the possible underlying mechanism. We discuss the multipole mechanisms first.

1. Multipole mechanisms

Following Dexter,[13] who first proposed the relevance of exchange and multipole interactions in invoking such ET processes, and Inokuti and Hirayama[14] who analyzed the expected rates of nonradiative transfer from donors to acceptors, we briefly outline the following. The interaction matrix element for nonradiative transfer between an excited donor ion (D^*) and a ground-state acceptor ion (A) can be written as

$$\langle D^* A | H_{DA} | D A^* \rangle , \tag{1}$$

where the operator H_{DA} represents an electrostatic interaction. The energy transfer rate is then given by

$$P_{DA} = 4\pi^2 c |\langle D^* A | H_{DA} | D A^* \rangle|^2 \int g_D(\tilde{\nu}) g_A(\tilde{\nu}) d\tilde{\nu} , \tag{2}$$

where $g_D(\tilde{\nu})$ and $g_A(\tilde{\nu})$ are the line-shape functions associated with the relevant emission and absorption transitions of donors and acceptors. For multipole interactions, the distance dependence of the ET rate can be expressed in the form

$$P_{DA}(R) = C R^{-S} , \tag{3}$$

where R is the separation between the two interaction ions and $S = 6$, 8, or 10 for d-d (dipole-dipole), d-q (dipole-quadrupole), and q-q (quadrupole-quadrupole) interactions, respectively. The constant C is given by

$$C_{(d\text{-}d)} = \frac{3e^4 f_D f_A}{8\pi^2 m^2 c^3 n^4 \tilde{\nu}^2} \int g_D(\tilde{\nu}) g_A(\tilde{\nu}) d\tilde{\nu} , \tag{4}$$

$$C_{(d\text{-}q)} = \frac{135\alpha e^4 f_D f_A}{32\pi^4 m^2 c^3 n^4 \tilde{\nu}^4} \int g_D(\tilde{\nu}) g_A(\tilde{\nu}) d\tilde{\nu} , \tag{5}$$

$$C_{(q\text{-}q)} = \frac{225\epsilon e^4 f_D f_A}{64\pi^6 m^2 c^3 n^4 \tilde{\nu}^6} \int g_D(\tilde{\nu}) g_A(\tilde{\nu}) d\tilde{\nu} , \tag{6}$$

where cgs units are used throughout, f_D and f_A are the relevant emission and absorption oscillator strengths, and α and ϵ are constants of order unity. The above expressions hold for electric multipole processes where n is the refractive index of the crystal ($n = 1.74$ for MgO). The expressions also hold for magnetic-electric multipole processes if n^4 is replaced by n^2 and magnetic multipole processes if replaced by unity.

If we assume a random distribution of ions and isotropic ET, the following expression is obtained for the shape of the decay curve:

$$^1T_{2g}(t) = \exp\left[-\frac{1}{\tau_0} t - \frac{4\pi}{3} \Gamma\left(1 - \frac{3}{S}\right) c C^{3/S} t^{3/S} \right] , \tag{7}$$

where τ_0 is the natural decay time of ions that do not undergo cross relaxation, i.e., the single-exponential decay time obtained from the dilute Ni^{2+}:MgO crystal and c is

the concentration expressed in ions/cm^3. A critical concentration, at which the average ion in the crystal will have the same probability of emitting a photon as cross relaxing with a nearby neighbor is defined as

$$c_0 = \left[\frac{3}{4\pi}\right](\tau_0 C)^{-3/S} . \tag{8}$$

A further assumption in the above treatment is that energy migration in the $^1T_{2g}$ excited state is negligible. Since the $^1T_{2g} \rightarrow {}^3A_{2g}$ emission band is Stokes shifted from the $^3A_{2g} \rightarrow {}^1T_{2g}$ absorption, this is likely a good approximation and therefore fulfills the conditions of the Inokuti-Hirayama model.[14]

The $^1T_{2g}$ decay curve at 2.0 K (lower trace Fig. 3) was therefore fitted to Eq. (7) with τ_0 fixed at 42 μs and C treated as an adjustable parameter. The fits obtained for d-d, d-q, and q-q interactions are given by the solid lines in Fig. 3. The best fit was obtained for the d-q mechanism, however, due to the closeness of the d-d and q-q fits, a critical comparison between the three multipolar mechanisms based solely on the quality of the fit is difficult. The best situation would have been to obtain the decay curve of a different concentration crystal exhibiting cross relaxation, and to find a consistency for the d-q mechanism. Since we had no other crystals available in the present study, we shall satisfy ourselves with analyzing the parameter values obtained for C and attempting to ascertain which might be the most appropriate. The best fits illustrated in Fig. 3 yielded the following values of C:

$$C_{(d\text{-}d)} = 8.2\times10^{-39}\ \text{cm}^6\text{s}^{-1} , \tag{9a}$$

$$C_{(d\text{-}q)} = 8.9\times10^{-53}\ \text{cm}^8\text{s}^{-1} , \tag{9b}$$

$$C_{(q\text{-}q)} = 1.4\times10^{-66}\ \text{cm}^{10}\text{s}^{-1} . \tag{9c}$$

From Eqs. (4)–(6), we can see that the only unknowns in C are the products of the emission and absorption oscillator strengths $f_D f_A$. Using the values of C in (9a)–(9c) and the overlap integral given in Sec. III we obtained the required oscillator strength products for all the possible magnetic dipole (md) and electric dipole (ed) or electric quadrupole (eq) processes, and these are collected together in Table I. Note that the relatively large value of the refractive index of MgO causes a difference of almost an order of magnitude between the required products $f_{\text{md}}f_{\text{md}}$ and $f_{\text{ed}}f_{\text{ed}}$. Although magnetic dipole processes are usually too weak to provoke energy transfer, we might expect them to be physically relevant in the special case of Ni^{2+}:MgO where we have a magnetic dipole-allowed $^3A_{2g} \rightarrow {}^3T_{2g}$ absorption. Also, we will not discount the possibility that quadrupole interactions may be relevant. As was pointed out in the original paper by Dexter,[13] even though quadrupole oscillator strengths are, in general, much smaller than dipole oscillator strengths, the probability of energy transfer through a dipole-quadrupole mechanism may be greater than for a dipole-dipole mechanism.

In the following discussion we will therefore attempt to calculate, either from experiment or theory, the relevant donor and acceptor oscillator strengths and see if the products obtained are in agreement with any of the required products in Table I. We begin with the magnetic dipole-dipole interaction. The md oscillator strength of the $^3A_{2g} \rightarrow {}^3T_{2g}$ absorption transition of Ni^{2+}:MgO is measured to be 2.3×10^{-6} from low-temperature spectra. We therefore would require a $^1T_{2g} \rightarrow {}^1E_g, {}^3T^a_{1g}$ md oscillator strength of 1.7×10^{-5} if we are to explain the cross relaxation by a magnetic dipole-dipole interaction. To calculate the md oscillator strengths of the latter inter-excited-state transitions, we diagonalized the crystal-field Hamiltonian of an octahedral d^8 configuration for all states. This procedure[15] included electrostatic, cubic, and spin-orbit interactions and yielded the best-fit parameters $B = 855\ \text{cm}^{-1}$, $C = 3550\ \text{cm}^{-1}$, $Dq = 830\ \text{cm}^{-1}$, and $\zeta = 650\ \text{cm}^{-1}$. The magnetic dipole transition moments were then obtained by calculation of the following matrix elements:

$$M_{ij} = \langle i | kl + 2s | j \rangle , \tag{10}$$

where i and j represent state wave functions obtained after diagonalization and k is an orbital reduction factor. The squares of the operator in Eq. (10) were then calculated for the relevant combinations of i's and j's for both the $^3A_{2g} \rightarrow {}^3T_{2g}$ absorption and the $^1T_{2g} \rightarrow {}^1E_g, {}^3T^a_{1g}$ emission. From the ratios of these transition moments and the experimental $^3A_{2g} \rightarrow {}^3T_{2g}$ oscillator strength, a md oscillator strength of 7.0×10^{-7} for the

TABLE I. Required and calculated oscillator strength products for multipole mechanisms.

	Required oscillator strength product[a]	Calculated oscillator strength product[b]
$f_{\text{md}}f_{\text{md}}$	3.9×10^{-11}	1.6×10^{-12}
$f_{\text{md}}f_{\text{ed}}$	1.2×10^{-10}	1.6×10^{-13} (D = md, A = ed)
		2.3×10^{-11} (D = ed, A = md)
$f_{\text{ed}}f_{\text{ed}}$	3.6×10^{-10}	2.3×10^{-12}
$f_{\text{md}}f_{\text{eq}}$	6.0×10^{-17}	1.0×10^{-20} (D = md, A = eq)
		1.7×10^{-15} (D = eq, A = md)
$f_{\text{ed}}f_{\text{eq}}$	1.8×10^{-16}	1.5×10^{-19} (D = ed, A = eq)
		1.7×10^{-16} (D = eq, A = ed)
$f_{\text{eq}}f_{\text{eq}}$	2.6×10^{-21}	1.0×10^{-23}

[a]From the values of C given in (9a)–(9c) and Eqs. (4)–(6).
[b]Products obtained from oscillator strengths of Table II.

$^1T_{2g} \rightarrow {}^1E_g, {}^3T^a_{1g}$ emission was obtained, as shown in Table II where all the oscillator strengths used in our discussion are collected. The calculated product falls short of the required product by a factor of ~ 25 and we can therefore rule out a magnetic dipole-dipole process to explain the cross relaxation.

In order to consider md-ed and ed-ed processes, we need ed oscillator strengths for both the absorption and emission transitions. Now, we we have already stated, the $^3A_{2g} \rightarrow {}^3T_{2g}$ absorption transition is md allowed and, from its very small temperature dependence,[5] we estimate that the ed contribution to this transition is at least an order of magnitude smaller than the md contribution. We therefore set an upper limit of 2.3×10^{-7} for its ed contribution. Experimentally, the ed oscillator strength of the $^1T_{2g} \rightarrow {}^1E_g, {}^3T^a_{1g}$ emission is difficult to measure, since it requires a knowledge of the branching ratios of all the radiative and nonradiative processes from $^1T_{2g}$. However, from a knowledge of ed oscillator strengths of Ni^{2+} O_h systems, it is probably safe to assume an upper limit of around 1×10^{-5}. With these upper limit values, we can see from Table I that the products obtained still fall short of the required $f_{\rm md}f_{\rm ed}$ and $f_{\rm ed}f_{\rm ed}$ products by almost an order of magnitude or greater, thus ruling out these mechanisms.

We now turn our attention to the notion that a dipole-quadrupole mechanism might be responsible for cross relaxation as the best fit shown in Fig. 3 does indeed seem to support. To do this we need quadrupole oscillator strengths for the absorption and emission transitions. The quadrupole tensor for a single electron has for its components xz, yz, xy which form a basis for T_{2g} in O_h symmetry. The $^3A_{2g} \rightarrow {}^3T_{2g}$ absorption, for which we are interested in estimating a quadrupole oscillator strength, is electric quadrupole forbidden in first order. However, the $^3A_{2g} \rightarrow {}^3T^a_{1g}$ is allowed and if we can estimate its quadrupole oscillator strength we can use the mixing coefficients obtained from the eigenvectors of our crystal-field calculation to estimate the former oscillator strength. Using the formalism of Griffith[16] we can write the following expression for the $^3A_{2g} \rightarrow {}^3T^a_{1g}$ electric quadrupole oscillator strength

$$f_{\rm eq}({}^3A_{2g} \rightarrow {}^3T^a_{1g}) = \frac{3\pi m\tilde{\nu}^3}{5hc^2} \left| \left\langle a\,{}^3T^a_{1g}1\xi \left| \sum_i x_i y_i \right| {}^3A_{2g}1a_2 \right\rangle \right|^2 , \quad (11)$$

where the operator represents the summation vector referring to the ith electron. Using the relationships given in Ref. 16,

$$|{}^3A_{2g}1a_2\rangle = |\theta^\dagger\epsilon^\dagger\rangle$$

and (12)

$$|{}^3T^a_{1g}1\xi\rangle = |\xi^\dagger\epsilon^\dagger\rangle ,$$

we obtain

$$f_{\rm eq}({}^3A_{2g} \rightarrow {}^3T^a_{1g}) = \frac{3\pi m\tilde{\nu}^3}{5hc^2} |\langle\xi|xy|\theta\rangle|^2 . \quad (13)$$

From the techniques given in Ref. 16, the matrix element is evaluated as

$$\langle\xi|xy|\theta\rangle = -\left[\frac{2}{7\sqrt{3}}\right]\overline{r^2} \quad (14)$$

and we finally obtain

$$f_{\rm eq}({}^3A_{2g} \rightarrow {}^3T^a_{1g}) = \frac{4\pi m\tilde{\nu}^3}{245hc^2}(\overline{r}^2)^2 . \quad (15)$$

For frequency $\tilde{\nu}=8000\ {\rm cm}^{-1}$ and adopting a value of 0.5 Å^2 for the Bohr radius $\overline{r}$, we obtain a value of 1.7×10^{-13} for the quadrupole oscillator strength of $^3A_{2g} \rightarrow {}^3T^a_{1g}$. Inspection of the mixing coefficients then gives a quadrupole oscillator strength for $^3A_{2g} \rightarrow {}^3T_{2g}$ of 1.5×10^{-14}.

For the case of the $^1T_{2g} \rightarrow {}^1E_g, {}^3T^a_{1g}$ emission, which is electric quadrupole allowed we can make use of the more general expression[17] since we know the md oscillator strength:

$$\frac{f_{\rm md}}{f_{\rm eq}} = \frac{(\mu_B/C)^2}{(e\overline{r}^2\pi/\lambda)^2} . \quad (16)$$

In expression (16), μ_B is the Bohr magneton and λ is the wavelength of the transition. This procedure yielded a value for the $^1T_{2g} \rightarrow {}^1E_g, {}^3T^a_{1g}$ electric quadrupole oscillator strength of 7.3×10^{-10}. Examination of the products obtained involving quadrupole interactions, which are given in Table I, shows that the mechanism involving a magnetic dipole transition on the acceptor ($^3A_{2g} \rightarrow {}^3T_{2g}$ absorption) accompanied by an electric quadrupole transition on the donor ($^1T_{2g} \rightarrow {}^1E_g, {}^3T^a_{1g}$ emission) provides a product almost 30 times greater than the one required to

TABLE II. Experimental and calculated oscillator strengths of relevant transitions used in cross-relaxation calculations.

	Magnetic dipole	Electric dipole	Electric quadrupole
$^3A_{2g} \rightarrow {}^3T_{2g}$ (absorption)	2.3×10^{-6}[a]	2.3×10^{-7}[c]	1.5×10^{-14}[e]
$^1T_{2g} \rightarrow {}^1E_g, {}^3T^a_{1g}$ (emission)	7.0×10^{-7}[b]	1.0×10^{-5}[d]	7.3×10^{-10}[e]

[a]From absorption spectrum.
[b]From magnetic dipole moments derived from crystal-field diagonalization.
[c]Upper limit based on temperature dependence of absorption.
[d]Upper limit based on typical values of ed oscillator strengths for $O_h Ni^{2+}$.
[e]Calculated values as explained in text.

explain the energy transfer. The ed-eq mechanism involving an ed absorption transition gives a product of 1.7×10^{-16} very close to the required value of 1.8×10^{-16}. However, we should bear in mind that our estimation of 2.3×10^{-7} for the ed oscillator strength of the $^3A_{2g}\rightarrow{}^3T_{2g}$ absorption was an upper limit. The other dipole-quadrupole and the quadrupole-quadrupole products are all 2 or more orders of magnitude less than the required values.

From the fact that the best fit was obtained for a dipole-quadrupole mechanism, and from the above calculation which appears to favor the md-acceptor–eq-donor interaction as the strongest, our data is consistent overall with this mechanism. Making use of Eq. (3), an average transfer time of around 30 ms is calculated for a 0.25 at. % Ni^{2+}:MgO crystal with an average Ni^{2+} ion separation of around 20 Å. With Eq. (2) we then calculate that this corresponds to an interaction strength H_{DA} of $\sim4\times10^{-3}$ cm^{-1} for an excited center and ground-state center separated by 20 Å. This extrapolates to a nearest-neighbor (2.1 Å) dipole-quadrupole interaction of ~40 cm^{-1}.

2. *Exchange mechanism*

For the case of an exchange interaction, we again use the formalism of Dexter[13] and assume an exponential R dependence:

$$H_{ex}=V_{ex}\exp(-R/a)\ . \tag{17}$$

With this expression we find the probability per s for energy transfer from D^* to A, a distance R apart, by an exchange mechanism is

$$P_{DA}(R)=\alpha\exp(-2R/a)\ , \tag{18}$$

where

$$\alpha=4\pi^2c|\langle D^*A|V_{ex}|DA^*\rangle|^2\int g_D(\tilde{\nu})g_A(\tilde{\nu})d\tilde{\nu}\ . \tag{19}$$

We can then obtain the following expression for the shape of the decay curve:

$$^1T_{2g}(t)=\exp\left[-\frac{1}{\tau_0}t-\frac{\pi a^3c}{6}g(\alpha t)\right]\ . \tag{20}$$

For the time regime in which we are interested, $g(\alpha t)$ can be approximated as

$$g(\alpha t)=(\ln\alpha t)^3+1.732(\ln\alpha t)^2+5.934(\ln\alpha t)+5.445\ . \tag{21}$$

A fit of Eq. (20) to the $^1T_{2g}$ decay transient in Fig. 3 yielded the parameters $\alpha=3.6\times10^6$ s^{-1} and $a=3.4$ Å. The fit, however, was not as good as the one obtained for the dipole-quadrupole mechanism. Using the experimental values of α and a and Eqs. (17) and (19), we obtain 3.9×10^{-3} cm^{-1} for the H_{ex} between the excited donor and ground-state acceptor 20 Å apart, which extrapolates to a nearest-neighbor value of 0.77 cm^{-1}.

To summarize, our calculations show that the dipole-dipole and quadrupole-quadrupole mechanisms do not appear to be strong enough to explain the energy-transfer data. The shape of the $^1T_{2g}$ decay curve is most consistent with a dipole-quadrupole mechanism and, according to the oscillator strengths we have derived, a md acceptor transition accompanied by an eq donor transition appears to provide the strongest interaction. However, the exchange mechanism, even though it did not provide such a good fit, still yielded reasonable parameter values and cannot be ruled out either from acting on its own or in conjunction with a dipole-quadrupole interaction of similar magnitude.

B. Assignments of Ni^{2+}-Ni^{2+} pairs

In order to identify the different types of Ni^{2+}-Ni^{2+} pairs and correlate them with the sharp lines observed in Fig. 4, we firstly consider the rocksalt structure of MgO. The dopant Ni^{2+} ions replace Mg^{2+} ions in the fcc lattice as shown in Fig. 5 where the two possible types of pair are illustrated. The nearest-neighbor (NN) pair has a 90° bridging geometry for Ni-O-Ni, while the next-nearest-neighbor (NNN) pair has a 180° arrangment. In this situation, the Kanamori-Goodenough rules[18,19] can be used to predict the sign of the orbital exchange parameters. For a d^8-d^8 metal ion pair with 180° bridging geometry (i.e., the NNN pair in Ni^{2+}:MgO) they predict a strong antiferromagnetic interaction. For a 90° arrangement, on the other hand (the NN pair), a ferromagnetic interaction is predicted.

The Ni^{2+} single ion has an orbitally degenerate $^3A_{2g}$ ground state; hence, the exchange interactions can be simply described by a Heisenberg operator of the form

$$\hat{H}_{ex}=-2J(S_1S_2)\ . \tag{22}$$

With $S_1=S_2=1$, the result is a Landé splitting pattern where the eigenvalues are given by

$$E(S)=-J[S(S+1)-4]\ , \tag{23}$$

where S is the total pair spin. For antiferromagnetic coupling this will result in three sublevels with $S=0,1,2$, where the $S=0$ level is lowest in energy and the energy separations are given by $2J$ and $4J$. For ferromagnetic coupling, J is positive and the spin sublevels are reversed in order. Since the pure material NiO, which has the same crystal structure as MgO, is an antiferromagnet with a Néel temperature of 520 K,[18] the Kanamori-Goodenough rules suggest that the dominant interaction is the strong 180° superexchange. The two peaks with the largest splitting at 7918 and 7883 cm^{-1} are therefore assigned to the NNN pair. The emitting level is assumed to be an $S=0$ state since the 7918-cm^{-1} peak is the most intense and this transition obeys the $\Delta S=0$ selection rule which is appropriate for an exchange-induced electric dipole mechanism.[20] The weaker band at 7883 cm^{-1} is assigned to the $S=1$ sublevel and since this transition has $\Delta S=1$ and can only occur by a single-ion mechanism; this explains why it is weaker than the $S=0$ level. A transition to the $S=2$ level is doubly spin forbidden and we failed to observe any peak corresponding to this sublevel at lower energy. From the assignments of the two lines at 7918 and 7883 cm^{-1} to $S=0$ and 1, respectively,

we therefore obtain a value for the exchange parameter $2J=-35\ \mathrm{cm}^{-1}$ for the NNN pair.

The splitting of the two bands at 7999 and 7994 cm^{-1} is an order of magnitude smaller than for the NNN pairs. These two peaks are assigned to the $S=2$ and 1 sublevels at a ferromagnetically coupled NN (90°) pair. If the emitting level in this case is an $S=2$ level, similar arguments as above can be applied to the observed intensities and we obtain $2J=2.5\ \mathrm{cm}^{-1}$ for the NN pair.

C. Energy transfer from $^3T_{2g}$

The results presented in Sec. III clearly indicate that, at low temperatures (2 K), energy transfer takes place from single ions to pairs. This follows from the observed rise of the NNN pair transients C and D shown in Fig. 6. The transient denoted by C was obtained after excitation into the broad vibronic sideband of the $^3A_{2g}\rightarrow{}^3T_{2g}$ absorption and presumably all Ni^{2+} species in the crystal, both single ions and pairs, are simultaneously excited. The large nonzero component at zero time is therefore a result of direct excitation of NNN pairs, after which energy transfer from single ions continues to feed the pairs slowly resulting in the observed rise. The simplest model to account for such a process is one in which the decay rate of the donors act collectively with an effective energy transfer rate W_{DA}. Neglecting back transfer, the rate of change of excited centers is given by

$$\frac{dN_D}{dt}=-W_DN_D-W_{DA}N_D\ , \tag{24}$$

$$\frac{dN_A}{dt}=-W_{DA}N_D-W_AN_A\ , \tag{25}$$

where N_D and N_A are the number of excited donors (single ions) and acceptors (NNN pairs), respectively, and W_D and W_A are the intrinsic decay rates of donors and acceptors, respectively. Integration of (24) and (25) yields the following expression for the decays of donors and acceptors:

$$N_D(t)=N_D(0)\exp[-(W_D+W_{DA})t]\ , \tag{26}$$

$$N_A(t)=N_A(0)\exp(-W_At)+N_D(0)\frac{W_{DA}}{(W_D+W_{DA})-W_A}\times\{\exp(-W_At)-\exp[-(W_D+W_{DA})t]\}\ . \tag{27}$$

With W_D fixed at the observed decay rate of 257 s^{-1} for single Ni^{2+} ions in the 0.11 at. % crystal, a fit of Eq. (27) to transient C of Fig. 6 was made. The parameters from the fit were $N_D/N_A=0.45$, $W_{DA}=754\ \mathrm{s}^{-1}$, and $W_A=270\ \mathrm{s}^{-1}$. The rise is therefore well described by a single exponential which seems to support the appropriate choice of the simple kinetic model. This can either be interpreted in terms of fast migration among single ions before transfer to pairs resulting in a collective transfer rate, or that each donor single ion occupies a fixed and similar lattice position with respect to the acceptors.

In a separate experiment, the Ni^{2+} single ions were selectively excited by excitation into the $^3A_{2g}\rightarrow{}^3T_{2g}$ zero-phonon absorption band with a narrow-band laser. The transient obtained for the NNN pair line at 7918 cm^{-1} using this excitation scheme is shown in trace D of Fig. 6. It contains no instantaneous component and is purely composed of pairs fed by energy transfer. The solid line through this transient was generated with Eq. (27) using the same parameters from the fit to transient C, with $N_A=0$.

We now turn our attention to the upper transients of Fig. 6 which were obtained by setting the monchromator to positions A and B of Fig. 4. These transients represent 0.25 at. % Ni^{2+}:MgO single-ion decays taken at slightly different positions within the inhomogeneous linewidth. If all the single ions in the crystal were equivalent and acted as donors, these transients would be single exponentials described by (26). Transient A clearly has a faster decay than B, and neither is a single exponential. The solid lines through A and B are fits to a modified version of (26) which includes a contribution from isolated single ions (SI) that are not capable of energy transfer

$$N(t)=N_{\mathrm{SI}}(0)\exp(-W_{\mathrm{SI}}t)+N_D(0)\exp[-(W_D+W_{DA})t]\ , \tag{28}$$

where N_{SI} is the number of isolated single ions. Fixing W_{SI} and W_D at 257 s^{-1} and W_{DA} at 754 s^{-1} yielded the ratios of isolated single ions to donor single ions $N_{\mathrm{SI}}/N_D=0.47$ and 1 for positions A and B, respectively. We therefore conclude that there is a slight energy mismatch between the isolated single ions and the donor single ions caused by the slightly different electron repulsion parameters of a single Ni^{2+} ion with a nearby pair .

V. CONCLUSIONS

We have shown that, at high concentrations of Ni^{2+} in MgO, two different excited states are involved in the transfer of excitation energy. Our calculations show the importance of the strong magnetic dipole nature of the $^3A_{2g}\rightarrow{}^3T_{2g}$ absorption in likely being involved in the mechanism of cross relaxation. Although our results do not rule out the possibility of an exchange interaction, it appears that an electric quadrupole donor and magnetic dipole acceptor mechanism is the highest probability process of all the possible multipolar mechanisms. In addition, we have identified two types of Ni^{2+} pairs and correlated the exchange coupling to NN (ferromagnetic) and NNN (antiferromagnetic) interactions. Energy transfer from Ni^{2+} single ions in the $^3T_{2g}$ excited state to Ni^{2+} pairs is also shown to be an important relaxation mechanism in crystals with high Ni^{2+} concentrations.

Finally, we remark that the present study has treated quite different interactions between Ni^{2+} ions, namely the excited-state–ground-state interactions of Sec. IV A compared to the purely ground-state–ground-state interactions of Sec. IV B. It is tempting to try to find some correlation between the parameter values we have obtained for both cases. If the exchange mechanism is indeed important for cross relaxation, we then have the

extrapolated value of 0.77 cm^{-1} for the exchange energy between nearest-neighbor excited- and ground-state Ni^{2+} ions to compare with values of $2J = 2.5$ or -35 cm^{-1} for ground-state nearest neighbors or next-nearest neighbors, respectively. However, it is dangerous to make such a direct comparison. The simple Heisenberg Hamiltonian of (22) no longer holds for the exchange between an ion in the orbitally degenerate $^1T_{2g}$ excited state and a ground-state ion. Using a simplified argument, however, we would conclude that the extrapolated H_{ex} of 0.77 cm^{-1} for the cross relaxation appears to be too low to support the exchange mechanism. This is because, according to quantum mechanics, exchange interactions have their origin in metal-to-metal or ligand-to-metal charge-transfer processes. The energies of such charge-transfer bands are generally assumed to lie well into the ultraviolet. Therefore, excited d states should be able to acquire more charge-transfer character and thus the exchange energy should be higher for the excited-state–ground-state interaction than for the ground-state–ground-state, and this is the opposite of what was found.

ACKNOWLEDGMENTS

We are grateful to Neil Manson for providing us with Ni^{2+}:MgO crystals and to Claude Daul for making his crystal-field programs available to us. This work is supported by National Science Foundation (NSF) Grant No. DMR-8717696.

*Also of the Department of Physics, University of Wisconsin, Madison, Wisconsin 53706.

[1]J. E. Ralph and M. G. Townsend, J. Phys. C **3**, 8 (1970).

[2]N. B. Manson, Phys. Rev. B **4**, 2645 (1971).

[3]W. E. Vehse, K. H. Lee, S. I. Yun, and W. A. Sibley, J. Lumin. **10**, 149 (1975).

[4]A. Mooradian and P. F. Moulton, Laser Focus **15**, 28 (1979).

[5]B. D. Bird, G. A. Osborne, and P. J. Stephens, Phys. Rev. B **5**, 1800 (1972).

[6]R. Moncorgé and T. Benyattou, Phys. Rev. B **37**, 9186 (1988).

[7]S. A. Payne, Phys. Rev. B **41**, 6109 (1990).

[8]J. Ferguson and H. Masui, J. Phys. Soc. Jpn. **42**, 1640 (1977).

[9]R. Moncorgé, F. Auzel, and J. M. Breteau, Philos. Mag. B **51**, 489 (1985).

[10]P. S. May and H. U. Güdel, Chem. Phys. Lett. **164**, 612 (1989).

[11]R. J. Tonucci, S. M. Jacobsen, and W. M. Yen, J. Lumin. **46**, 155 (1990).

[12]G. Grinvalds and N. A. Mironova, Phys. Status Solidi B **99**, K101 (1980).

[13]D. L. Dexter, J. Chem. Phys. **21**, 836 (1953).

[14]M. Inokuti and F. Hirayama, J. Chem. Phys. **43**, 1978 (1965).

[15]The crystal-field program is outlined in S. M. Jacobsen, H. U. Güdel, and C. A. Daul, J. Am. Chem. Soc. **110**, 7610 (1988).

[16]J. S. Griffith, *The Theory of Transition Metal Ions* (Cambridge University, Cambridge, 1961).

[17]B. Henderson and G. F. Imbusch, *Optical Spectroscopy of Inorganic Solids* (Oxford University, New York, 1988).

[18]J. B. Goodenough, *Magnetism and the Chemical Bond* (Interscience, New York, 1976).

[19]J. Kanamori, J. Phys. Chem. Solids **10**, 87 (1959).

[20]K. Gondaira and Y. Tanabe, J. Phys. Soc. Jpn. **21**, 1527 (1966).